Transit Met Chem (2017) 42:57–67
DOI 10.1007/s11243-016-0107-7

Rhodium(I) macrocyclic and cage-like structures containing diphosphine bridging ligands

Julià Arcau[1] · Montserrat Ferrer[1] · Elisabet Aguiló[1] · Laura Rodríguez[1]

Received: 26 October 2016 / Accepted: 24 November 2016 / Published online: 3 December 2016

Abstract Three series of rhodium organometallic complexes, mono-(**1c, 2c, 5c, 6c**), di-(**1a-6a**) and tetranuclear (**1b, 5b, 6b**), containing six different diphosphines 1,1′-bis (diphenylphosphino)methane or dppm (**1**), 1,2-bis(diphenylphosphino)ethane or dppe (**2**), 1,4-bis(diphenylphosphino)butane or dppb (**3**), bis(diphenylphosphino)acetylene or dppa (**4**), 1,2-bis(diphenylphosphino)benzene or dppbz (**5**) and 4,5-bis(diphenylphosphino)-9,9′-dimethylxanthene or xantphos (**6**) were successfully synthesised. These Rh(I) complexes were characterised by conventional techniques. The influence of the flexibility/rigidity of these P-donor ligands was carefully analysed, including their effect on both synthesis and catalysis. The luminescent properties of the dinuclear and tetranuclear complexes were investigated, and only those containing dppa, dppbz and xantphos displayed luminescence. Structures of the dinuclear complexes were modelled by using DFT methods in order to elucidate the most reasonable conformation. The different types of complexes were applied in the catalytic hydrogenation of (*E*)-4-phenylbut-3-en-2-one, showing high activity and similar catalytic behaviour. No cooperative effect could be inferred.

Electronic supplementary material The online version of this article (doi:10.1007/s11243-016-0107-7) contains supplementary material, which is available to authorized users.

✉ Laura Rodríguez
laura.rodriguez@qi.ub.es

[1] Departament de Química Inorgànica i Orgànica, Secció de Química Inorgànica, Universitat de Barcelona, Martí i Franquès 1-11, 08028 Barcelona, Spain

Introduction

The use of transition metal-based self-assembly processes has emerged as one of the most efficient ways to build artificial supramolecular structures [1–3]. Typically, a metal complex with two or more available coordination sites is reacted with an appropriately designed multifunctional ligand to give the product in one step in high yield.

Square-planar Pd(II) and Pt(II) complexes have been commonly used to prepare metallosupramolecules which contain square or near orthogonal angles in their geometries [1–8]. However, other metals have also been used in these reactions. In particular, Rh(I) and Ir(I) units have been explored in the synthesis of bi- [9–14] and three-dimensional compounds [15–18], they are of great interest due to their luminescent behaviour [19] and their potential catalytic activity [20–25] and they could also be very useful in molecular recognition studies [26, 27], among others.

In recent years, bimetallic complexes have been used in homogeneous catalysis as an effective tool for promoting organic transformations [28, 29]. Bimetallic catalysts can display cooperative effects, because of the proximity between the metal centres, leading to reactivities and selectivities that cannot be attained using their corresponding monometallic counterparts [30, 31].

Over the last few decades, bidentate ligands have been widely employed to improve selectivities, activities and stabilities of metal-complex-based homogeneous catalysts [32–35]. The key to optimise the performance of a certain species in a catalytic reaction is to adjust the electronic and steric properties together with the topology exhibited by the ligands.

The use of binucleating ligands with ligand isolated donor sets is one of the more recent developments where two metal centres are held in close proximity to

cooperatively catalyse a given organic transformation [31]. Cooperative effects that have been observed in bimetallic systems usually occur through electronic and/or spatial interactions. In particular, concerning the reactivity of group 9 bimetallic catalysts, it is important to underline the work reported by Stanley and co-workers with a highly selective and active dirhodium hydroformylation catalyst, [Rh_2(norbornadiene)(P4)], where P4 is the binucleating tetraphosphine-based ligand, ($Et_2PCH_2CH_2$)(Ph)PCH_2-P(Ph)($CH_2CH_2PEt_2$) [36]. Another example was shown by Messerle and co-workers with a dual metal catalyst system (Rh and Ir) using cationic Rh(I) and Ir(I) complexes of the type [M(bpm)$(CO)_2$]$BArF_4$ (where M = Rh or Ir, bpm = *bis*(1-pyrazolyl)methane, and $BArF_4$ = *tetrakis*[3,5-*bis*(trifluoromethyl)-phenyl]borate) which is observed to be a highly efficient catalyst for the two step intramolecular dihydroalkoxylation reaction of alkyne diols in the formation of spiroketals [37]. The two metal centres worked cooperatively to provide greater efficiencies than the individual monometallic complexes for the concurrent cyclisation of alkyne diols.

Van Leeuwen and co-workers claimed the involvement of bimetallic catalytic species using wide bite angle diphosphine ligands, in particular in carbonylation reactions [38, 39].

For all the reasons above, we decided to go on with our previous work based on the synthesis of bi- and three-dimensional rhodium structures containing diphosphine ligands as linkers between metal atoms [40]. Their catalytic behaviour in hydrogenation reactions was analysed, and the possible cooperative effects on these processes was studied and compared with the parent mononuclear rhodium complexes.

Results and discussion

Synthesis of rhodium dinuclear complexes

[RhCl$(CO)_2]_2$ was reacted with six different diphosphines **1–6** (Rh:P = 1:2) in dichloromethane at room temperature for 1 h (Scheme 1). The reaction was monitored by ^{31}P-NMR until the disappearance of the free diphosphine signal, which was ca. 40–60 ppm downfield shifted upon coordination to the metal atom. The corresponding dinuclear complexes [RhCl(CO)]$_2$(μ-diphos)$_2$ (**1a–6a**) were obtained in high yields after concentration of the solution and precipitation with hexane.

Complexes **1a** and **3a** were previously described following different synthetic procedures [41–43]. Evidence for the proposed structures was obtained from IR, ^{1}H-NMR and ^{31}P-NMR spectroscopy and MS spectrometry. ^{31}P-NMR spectra present different profiles due to the existence of different isomers and their relative stabilities as depicted in Fig. 1. **4a** displayed two set of signals with different intensities, showing close chemical shifts (24.0 and 24.6 ppm) and the same coupling constant value (J(P-Rh) = 124 Hz). This behaviour has been already reported in the literature for closely related dinuclear rhodium derivatives [44] and attributed to the existence of different conformational isomers arising from the relative disposition of the phosphine backbones (chair/boat or parallel/antiparallel in Figs. 2, 3) isomers and also from the relative orientation of the carbonyl and chloride ligands in both rhodium centres (*syn* and *anti* isomers in Figs. 2, 3).

Some broadening of the signals was only observed for **1a** and could be due to a dynamic process that involves the coordination–decoordination of the diphosphines, as previously observed for its analogue three-dimensional complex **1b** [40].

The sharp and well defined doublet exhibited by **2a**, **5a**–**6a** could be due to the fact that these diphosphines form exclusively one complex in solution, or that several isomers exist in a fast equilibrium at the temperature of study.

Structure optimisation of the dinuclear complexes

As indicated above, a wide range of different conformations could be plausible for our face-to-face (*trans*-P) complexes depending both on the *syn/anti* or *cis/trans* (only for **4a**) disposition of the chloride and carbonyl ligands coordinated to the metal atoms and the relative arrangement of the backbone chain of the diphosphine with respect to an imaginary Rh–Rh edge (chair/boat for complexes **1a** and **4–6a** or parallel/antiparallel for **2a** and **3a**).

In order to find out the different possible isomers and the most stable in each case, we have performed theoretical calculations at the DFT level, using the RB3LYP hybrid functional (see "Experimental section"). The optimised structures are displayed in Figures S1–S6, and the calculated minimum energy in all cases is shown in Table 1.

Inspection of Table 1 shows a clear dependence of the nature of the diphosphine upon the stability of the corresponding isomers. However, the obtained values do not allow establishing a direct correlation between length, bulkiness and/or flexibility of the phosphine backbone chain and the energetically favoured isomer. In spite of this, a general preference for the *anti* disposition of the chloride and carbonyl ligands is observed although in some cases the difference between both conformations is too small to be considered reliable (see for example **4a** boat and **6a** chair).

The rhodium atom presents, in all cases, a square-planar geometry and the inner cavities are observed to be in the range ca. 3.5 × 6.3 Å for **1a**, 5.1 × 5.6 Å for **2a**, 7.2 × 5.4 Å for **3a**, 3.0 × 5.1 Å for **5a** and 4.1 × 7.1 Å

Scheme 1 Synthesis of dinuclear complexes **1a**–**6a**

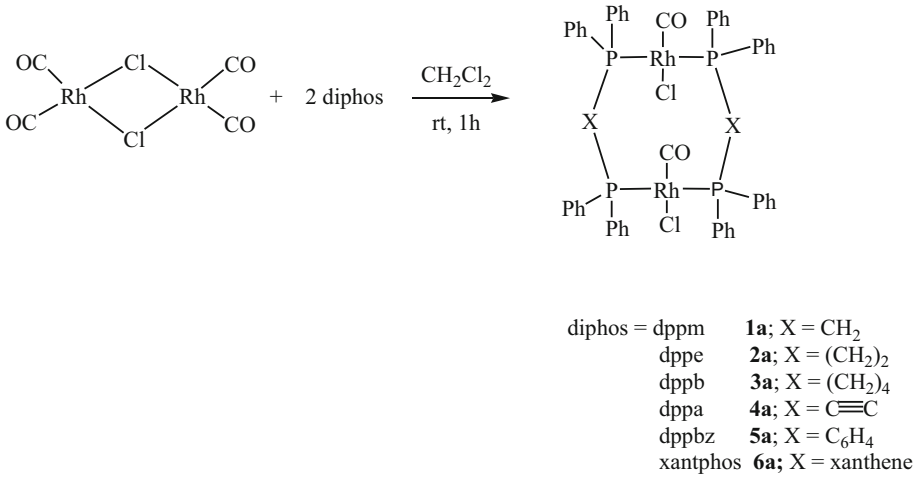

Fig. 1 ^{31}P-NMR spectra of **1a**, **4a** and **6a** in $CDCl_3$

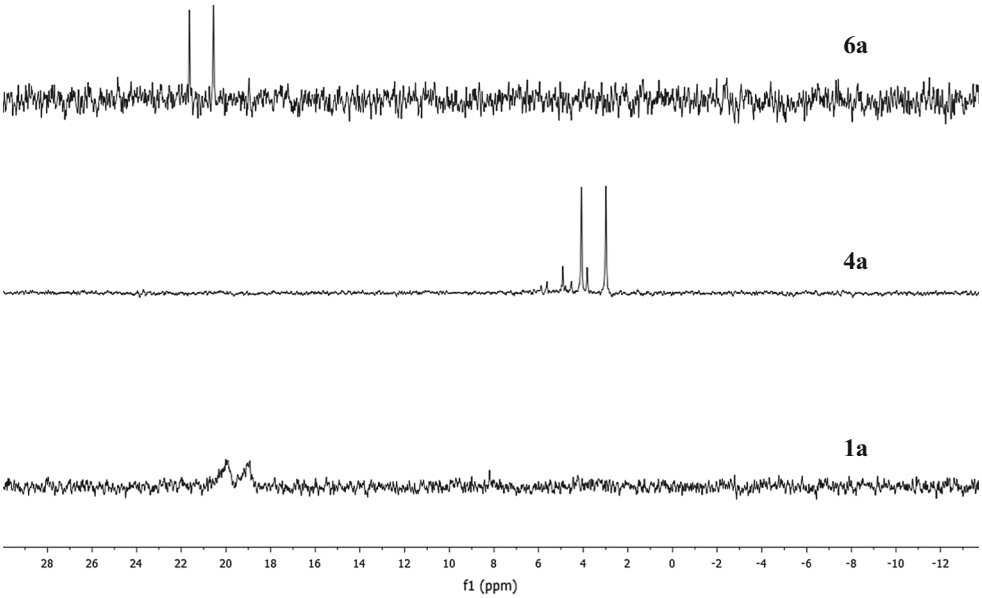

for **6a** for all possible conformations. A particular case is **4a** whose cavity presents a completely different size in the case of chair conformation (3.4 × 7.5 Å) and boat (5.3 × 5.4 Å). Moreover, the only square-like cavity is the one corresponding to the acetylide derivative **4a**, in boat conformation.

Synthesis of rhodium tetranuclear complexes

Following the same experimental procedure previously reported by some of us [40] (Scheme 2), we planned the synthesis of different cage-like rhodium structures. Our main goal was the formation of new three-dimensional complexes with different inner size cavities in order to explore their influence on different applications, such as catalysis.

$[RhCl(CO)_2]_2$(μ-4,4′-bipy) was reacted with the corresponding diphosphine (Rh:P = 1:2) in dichloromethane for 1 h. Actually compounds **1b** [40], **5b** and **6b** were efficiently isolated, while the use of the other diphosphines (dppe, dppb, dppa) did not give rise to the formation of the desired products. The high rigidity of the dppa probably prevents the cage-type structure and the high flexibility of dppe and dppb favours the formation of oligomers.

^{31}P-NMR spectra of **5b** and **6b** complexes exhibit one broad doublet centred at 20–60 ppm with a Rh–P coupling constant of ca. 135 Hz. The value of these coupling constants is in the same range as that previously reported for **1b** [40].

IR spectra show more complex ν(C≡O) stretching vibration patterns with respect to the two IR bands observed for the precursor, $[RhCl(CO)_2]_2$(μ-4,4′-bipy) (Figures S7 and S8) [40]. Each band splits into two with an additional lower energy vibration. This shift is in agreement with a higher retro-donation effect from the rhodium centre to the antibonding molecular orbital of the carbonyl

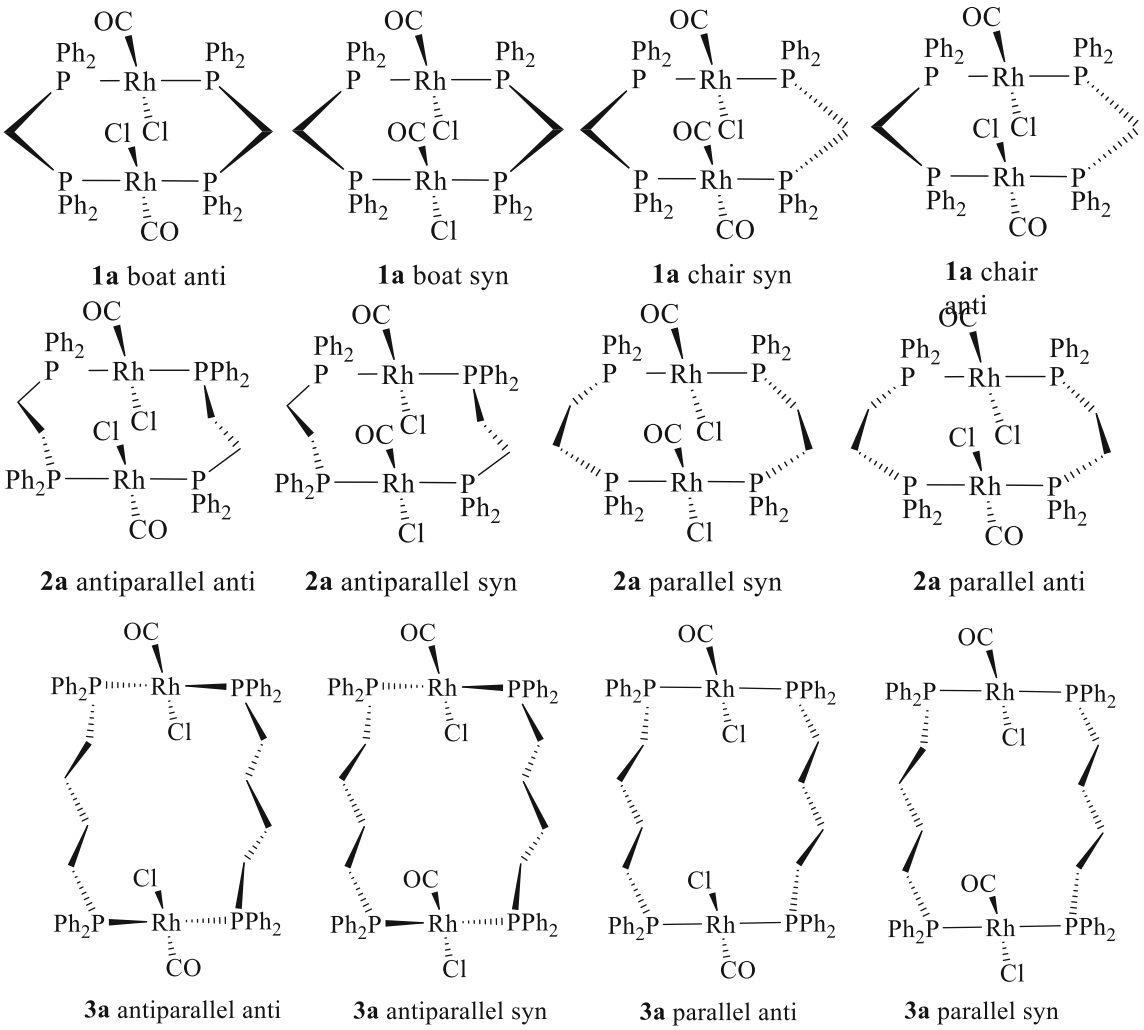

Fig. 2 Different possible conformers expected for **1a**–**3a** complexes

ligand because of the loss of one CO ligand upon diphosphine coordination. Maldi/TOF mass analyses evidenced peaks consistent with the tetranuclear structure.

Photophysical characterisation

Absorption and emission spectra of complexes **1a**, **2a**, **4a**–**6a, 1b, 5b** and **6b** were recorded at 1×10^{-5} M in dichloromethane. The results are summarised in Table 2; Figs. 4 and 5.

The spectra of both bimetallic and tetrametallic complexes are dominated by strong absorption bands attributed to intraligand (IL) $\pi \rightarrow \pi^*$ transitions, with diphosphine-based $\pi \rightarrow \pi^*$ transitions in the near-UV region between 280 and 300 nm along with a relatively weak, broad band in the visible range (between 350 and 450 nm). The broad visible bands are similar to the metal-to-ligand charge-transfer (MLCT) transitions observed in rhodium complexes containing π-acceptor ligands [45, 46], in which the charge-transfer character stems from interactions between filled metal *d* orbitals and antibonding ligand π^* orbitals.

The MLCT transition is observed to be less favoured for the tetrametallic derivatives, being only clearly defined for the dppbz derivative, **5b**, probably due to the higher aromaticity and electron deficiency of the system due to the presence of the benzene unit.

The only emissive dinuclear species are **4a** and **6a** (dppa and xantphos derivatives, Fig. 6). Excitation spectra collected at the emission maxima match the lowest energy absorption band being indicative of an intraligand emission origin. It should be noticed that, as displayed in Fig. 6, the emission spectrum of **4a** presents two different bands. The vibronically well-resolved highest energy emission band is in agreement with the involvement of the acetylene group on this transition. The broad structureless lowest energy band can be tentatively attributed to metal centred transitions, since $d\sigma^* \rightarrow p\sigma$ excited states are common for dinuclear Rh(I) complexes coordinated by bidentate ligands [47].

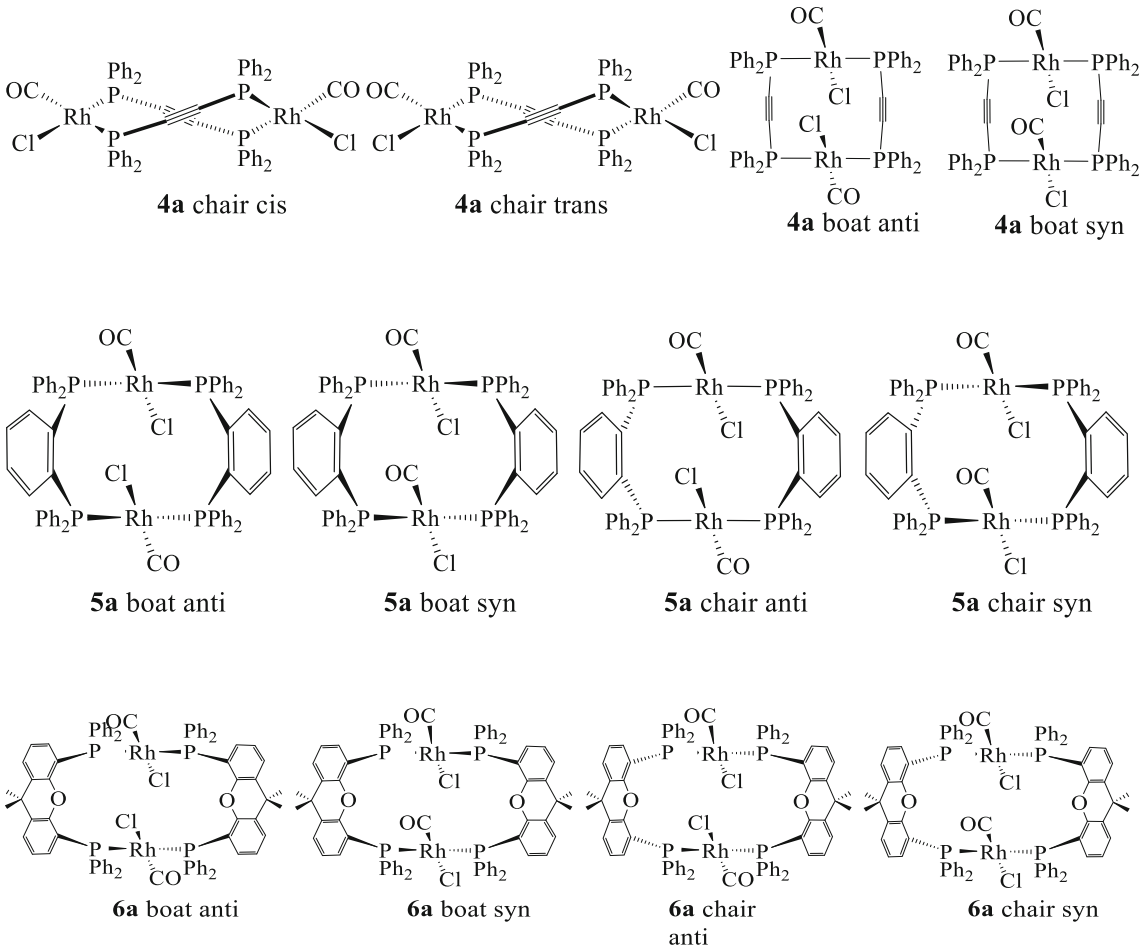

Fig. 3 Different possible conformers expected for **4a**–**6a** complexes

Compounds **1b** and **6b** (dppm and xantphos derivatives) displayed a broad luminescence at ca. 350 nm upon excitation the samples at the intraligand absorption band (Fig. 7). The small Stokes' shift (ca. 5000 cm^{-1}) suggests a singlet emissive IL origin state. An additional lower energy emission is observed for **6b** when the sample is excited at the MLCT transition being indicative of the different origin transitions. Excitation spectra collected at the maxima are in agreement with these assignments (Figure S9–S10). No emission was displayed by complex **5b**.

Synthesis of rhodium mononuclear complexes

Mononuclear derivatives were also synthesised in order to compare the catalytic behaviour of the different complexes. For this, the reaction of $[RhCl(CO)_2]_2$ with the appropriate diphosphine in stoichiometric conditions (after extraction of the chloride ligand by addition of silver triflate) was applied to give the monomeric species **1c**, **2c**, **5c** and **6c** (Scheme 3).

The corresponding reaction with dppb gave rise to the formation of different species in equilibrium whose ^{31}P-NMR signals showed similar chemical shifts, preventing the isolation of pure **3c**. Moreover, the rigidity of the alkynyl group of the diphosphine dppa prevents the diphosphine from acting as a chelating ligand and consequently precludes the formation of the mononuclear complex **4c** [45, 49].

IR spectra of the isolated complexes, in particular the region corresponding to $\nu(C\equiv O)$ absorptions, revealed the expected *cis*-CO arrangement in agreement with the reported data [38, 48].

Catalytic hydrogenation

The dinuclear complexes **1a**, **2a** and **4a**–**6a** were used as catalytic precursors in the hydrogenation reaction of the polyfunctional substrate (*E*)-4-phenylbut-3-en-2-one, in order to analyse their ability towards the reduction of the different groups present on the same substrate. **3a** was not used for this purpose since it was observed to decompose

Table 1 Calculated minimum energies for the different isomers of **1a–6a** compounds

Compound	Energy (kcal/mol)	
1a chair	*syn*	***anti***
	16.7	**0.0**
1a boat	*syn*	*anti*
	4.5	13.9
2a antiparallel	*syn*	*anti*
	6.4	14.3
2a parallel	*syn*	***anti***
	10.7	**0.0**
3a antiparallel	***syn***	*anti*
	0.0	12.1
3a parallel	*syn*	*anti*
	6.2	7.3
4a chair	*cis*	*trans*
	8.2	11.6
4a boat	*syn*	***anti***
	0.9	**0.0**
5a chair	*syn*	*anti*
	14.3	1.7
5a boat	*syn*	***anti***
	3.4	**0.0**
6a chair	*syn*	***anti***
	1.8	**0.0**
6a boat	*syn*	*anti*
	11.6	10.7

The most stable isomer (considered to have an energy of 0.0 kcal/mol) is highlighted in bold

rapidly in solution. Under the conditions indicated in Scheme 4, we could not observe important differences among the different Rh(I) complexes leading to full conversion (entries 1–5 in Table 3), except for **4a** which was less active (42% conversion, entry 3), probably due to an induction period corresponding to the hydrogenation of the C≡C triple bond present in the ligand skeleton, leading to the same catalytic system generated by **2a**. As expected [50], the hydrogenation mainly gave 4-phenylbutan-2-one (**A** in Scheme 4) in all the cases, being **6a** the most active system (able to hydrogenate the aromatic ring), which gave up to 14% of 4-cyclohexylbutan-2-one (entry 5), certainly formed from the hydrogenation of the non-conjugated compound **A**.

The system **1a** was the only one giving butylcyclohexane (**E** in Scheme 4) as by-product coming from the hydrogenative dehydration process of alcohol **D**.

In order to selectively attain one hydrogenated product, milder conditions were applied. Actually, 4-phenylbutan-2-one, **A**, was exclusively obtained under 5 bar of dihydrogen for 3 h of reaction (entry 6). Using the most active catalytic system, **6a**, under hasher conditions (at 80 °C or 40 bar H_2), no differences in the reactivity were observed (entry 5 vs. 7 and 8). With a higher load of catalyst and longer time, only **A** and **B** were obtained in a ratio of 77:23 (entry 9). The highest amount of **B** was obtained under 40 bar H_2 for 24 h (entry 10).

We also tested the tetranuclear complexes **1b** and **6b**. Xanthphos-based complex (**6b**) was slightly more active than **1b**, giving 92% of **A** and 8% of **C**, while **1b** led exclusively to the formation of **A**. Both catalytic trends are similar to those obtained with the corresponding dinuclear complexes, **1a** (under smooth conditions) and **6a,** respectively, (entries 5–6 vs. 11–12), pointing to a lower activity of the tetranuclear systems in comparison with the dinuclear ones.

The monometallic complex **2c** used as catalytic precursor, gave the same reactivity trend compared to the related bimetallic system **2a** (entry 13 vs. 2), without observing any influence concerning the presence of the chloride anion, present in **2a** [51]. The similar reactivity exhibited by the dinuclear complexes **1a**, **2a**, **5a** and **6a** and the monometallic complex **2c**, together with the lower activity of the tetranuclear complexes **1b** and **6b**, seems to suggest that the active catalytic species are mononuclear complexes generated in situ under catalytic conditions from the corresponding dinuclear ones.

Conclusions

The reaction of six different diphosphines with Rh(I) organometallic precursors led to the formation of five new dinuclear (**1a**, **2a**, **4a–6a**) and two tetranuclear (**5b**, **6b**) complexes. The use of the highly flexible dppb ligand precluded the formation of the complexes in pure form and rapid decomposition was observed in solution. The use of more rigid diphosphines (dppbz and xantphos) favoured the formation of three-dimensional cage-like derivatives.

The compounds displayed very weak emissions in dichloromethane with some intraligand luminescence observed for **4a**, **6a**, **1b** and **6b** and an additional ^{3}MLCT band for **6b**.

Theoretical calculations at density functional level (DFT) carried out to know the most stable conformation of the dinuclear complexes have shown a clear influence of the backbone of the diphosphine on the stability of the different conformers.

Mono-, di- and tetrametallic complexes were assayed as catalytic precursors for the hydrogenation of (*E*)-4-phenylbut-3-en-2-one. The similar behaviour observed between polynuclear and monometallic complexes suggests that the active catalytic species are mononuclear

Scheme 2 Synthesis of tetranuclear complexes **1b**, **5b** and **6b**

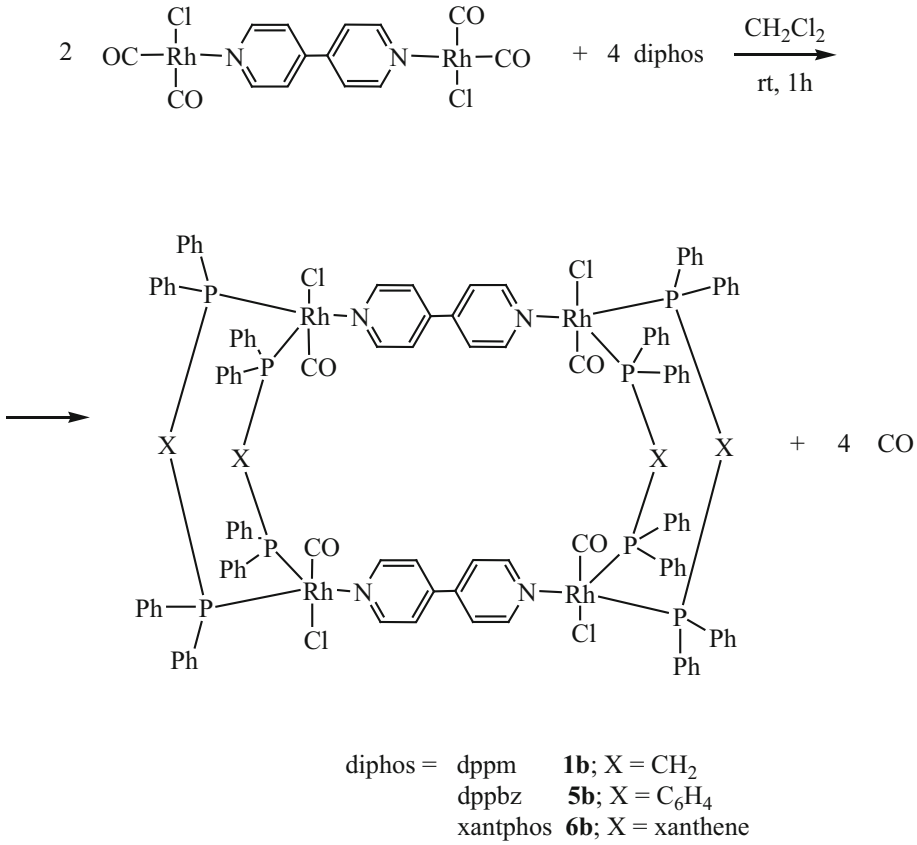

Table 2 Absorption and emission wavelengths (nm) of complexes **1a–6a** (λ_{exc} = 280 nm) and **1b–6b** (λ_{exc} = 274 nm) at 1×10^{-5} M concentration

Compounds	Absorption ($\varepsilon \times 10^{-3}$, M^{-1} cm^{-1})	Emission (CH_2Cl_2, 298 K)
1a	443 (5.8), 324 (6.1), 263 (27.2)	–
2a	390 (5.6), 343 (7.1), 275 (36.1)	–
3a	375 (3.21), 328 (5.4), 254 (31.2)	–
4a	270 (31.3)	340, 410
5a	428 (4.1), 325 (12.5), 272 (37.6)	–
6a	331 (5.0), 283 (24.0)	335
1b	335sh (7.1), 285 (45.9)	335
5b	428 (4.6), 325 (14.3), 265 (58.6)	–
6b	335sh (12.9), 280 (37.8)	335, 415[a]

[a] λ_{exc} = 333 nm

moieties generated under the catalytic conditions used in these studies.

Experimental section

General

All manipulations were performed under prepurified N_2 using standard Schlenk techniques. All solvents were distilled from appropriate drying agents. The complexes $[RhCl(CO)_2]_2$ [49], $[RhCl(CO)_2]_2$(μ-bipy) [40], 1,1′-bis(diphenylphosphino) methane (dppm) [52], 1,2-bis(diphenylphosphino)ethane (dppe) [52] 1,4-bis(diphenylphosphino)butane (dppb) [52], $[RhCl(CO)]_2$(μ-dppm)$_2$ [53] and $([RhCl(CO)]_2$(μ-4,4′-bipy))$_2$(μ-dppm)$_4$ (**1b**) [40] were synthesised as described previously. The compounds 4,4′-bipyridine (Avocado, 98%), *trans*-4-phenyl-3-butene-2-one (Janssen Chimica, 99%), 1,2-bis(diphenylphosphino)-acetylene (dppa), 4,5-bis(diphenylphosphino)-9,9′-dimethylxanthene (xantphos), 1,2-bis(diphenylphosphino)benzene (dppbz) were used as received.

Infrared spectra were recorded on an FTIR 520 Nicolet spectrophotometer. $^{31}P\{^1H\}$-NMR [δ(85% H_3PO_4) = 0.0 ppm] and ^{1}H-NMR [δ(TMS) = 0.0 ppm] spectra were

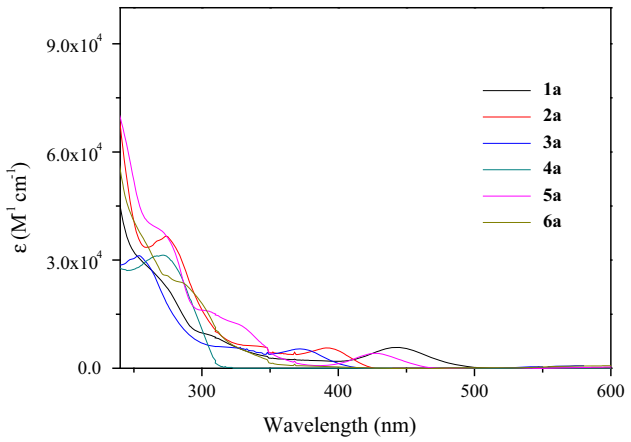

Fig. 4 Absorption spectra of the dinuclear complexes (**1a**, **2a**, **4a**–**6a**) at 1×10^{-5} M in dichloromethane

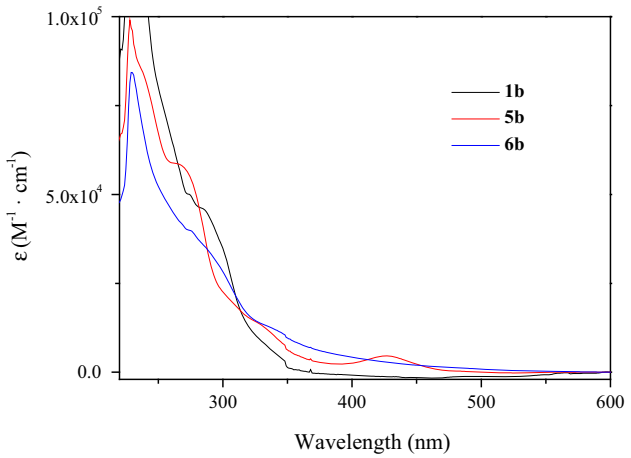

Fig. 5 Absorption spectra of **1b**, **5b** and **6b** complexes at 1×10^{-5} M in dichloromethane

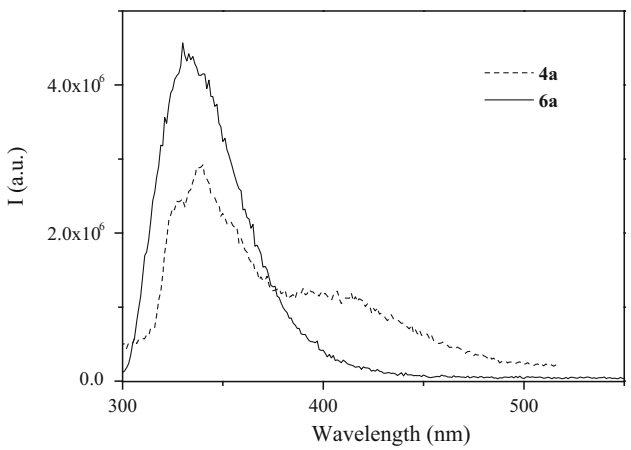

Fig. 6 Emission spectra of **4a** (*dashed line*) and **6a** (*solid line*) in dichloromethane solution (*dashed line*) upon excitation the samples at 280 nm

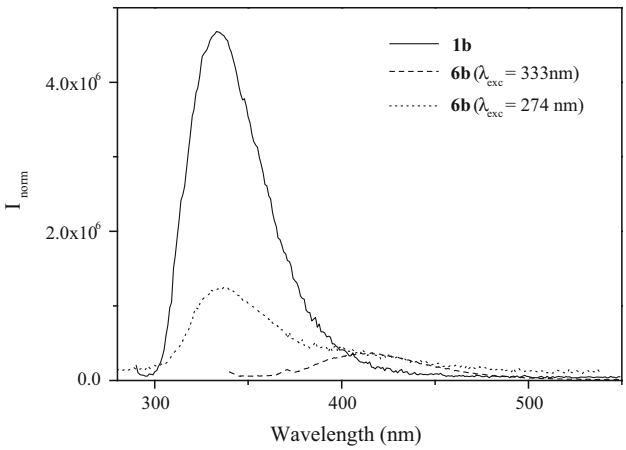

Fig. 7 Emission spectra of **1b** (*solid line*) and **6b** in dichloromethane solution (*dashed* and *dotted line*)

obtained on a Bruker DXR 250, Varian Inova 300 and Varian Mercury 400 spectrometers. ES(+) mass spectra were recorded on a Fisons VG Quatro spectrometer. Absorption spectra were recorded on a Varian Cary 100 Bio UV-spectrophotometer and emission spectra on a Horiba–Jobin–Yvon SPEX Nanolog spectrofluorimeter. GC analyses were carried out on an Agilent GC6890 with a flame ionisation detector, using an SGE BPX5 column composed by 5% of phenylmethylsiloxane. ES(+) mass spectra were recorded with a Fisons VG Quatro spectrometer. Maldi/TOF spectra were recorded on a Maldi Tof Voyager DE STR (Applied Biosystems) instrument.

Molecular modelling was carried out using Spartan'10 V1.1.0 for Mac as software. DFT calculations were carried out with the Spartan software using the B3LYP hybrid functional [54, 55]. The basis set was chosen as follows: for Rh LANL2DZ was used [56, 57] while for the remaining atoms the 6–31G basis [58] was used. The structures were previously optimised at MM+ molecular mechanics level.

Synthesis and characterisation

Synthesis of $[RhCl(CO)]_2(\mu\text{-dppm})_2$ **(1a)** Similar procedure previously described in the literature [53] was followed, but dichloromethane instead of cyclohexane was used as solvent. Yield: 74%. ^{31}P-NMR (121.42 MHz, 298 K, $CDCl_3$): 19.6 ppm (*d*, ^{1}J(Rh-P) = 115 Hz). ^{1}H-NMR (300 MHz, 298 K, $CDCl_3$): 7.67–7.27 (*m*, 40H, Ph), 3.96 (br, 4H, P–C*H*$_2$–P). ESI–MS(+) *m/z*: 1102.9 ($M + H^+$, calc.: 1102.5), 1045.0 ($M - 2CO + H^+$, calc.: 1046.1), 1010.0 ($M - 2CO - Cl^-$, calc.: 1010.0). IR (KBr, cm^{-1}) 1970s, $\nu(C\equiv O)$.

Synthesis of $[RhCl(CO)]_2(\mu\text{-dppe})_2$ **(2a)** A dichloromethane solution (5 mL) of dppe (103 mg, 0.26 mmol)

Scheme 3 Synthesis of monometallic complexes **1c**, **2c**, **5c** and **6c**

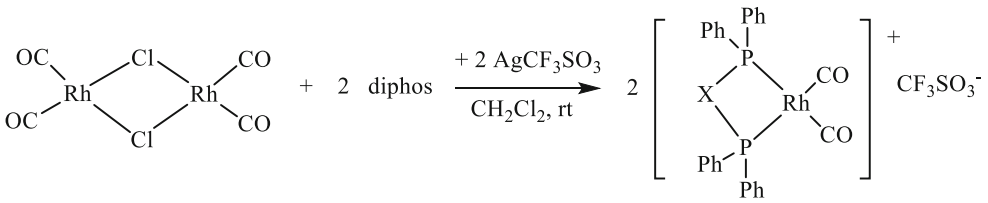

diphos = dppm **1c**; X = CH_2
dppe **2c**; X = $(CH_2)_2$
dppbz **5c**; X = C_6H_4
xantphos **6c;** X = xanthene

Scheme 4 Hydrogenation of (*E*)-4-phenylbut-3-en-2-one catalysed by Rh(I) complexes

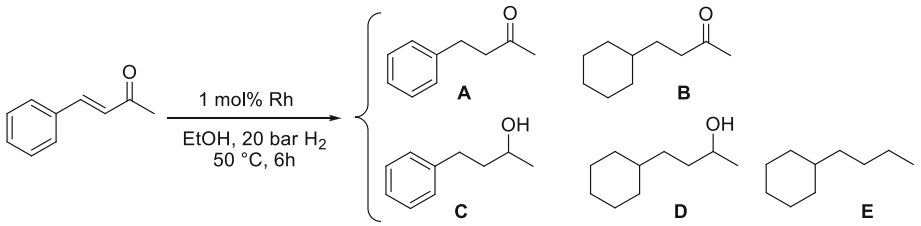

Table 3 Hydrogenation of (*E*)-4-phenylbut-3-en-2-one catalysed by polynuclear Rh complexes

Entry	Complex	Selectivity (%)[a] **A/B/C/D/E**
1	**1a**	87/4/7/–/2
2	**2a**	85/8/7/–/–
3[b]	**4a**	95/5/–/–/–
4	**5a**	88/5/7/–/–
5	**6a**	82/14/4/–/–
6[c]	**1a**	100/–/–/–/–
7[d]	**6a**	85/13/2/–/–
8[e]	**6a**	86/12/2/–/–
9[f]	**6a**	77/23/–/–/–
10[g]	**6a**	48/49/3/–/–
11	**1b**	100/–/–/–/–
12	**6b**	92/8/–/–/–
13	**2c**	85/9/6/–/–

Conditions: 1 mmol of (*E*)-4-phenylbut-3-en-2-one, 0.01 mmol of Rh, 20 bar H_2, 20 mL of ethanol, 50 °C, 2 h. Full conversion for all the systems except for **4a**

[a] Determined by GC and ^{1}H NMR using decane as internal standard

[b] 42% conversion

[c] Under 5 bar H_2 for 3 h

[d] At 80 °C

[e] Under 40 bar H_2

[f] 0.02 mmol of Rh for 24 h

[g] Under 40 bar H_2 for 24 h

was added to a solution (5 mL) of $[RhCl(CO)_2]_2$ (50 mg, 0.13 mmol) in the same solvent. After 1 h of stirring the bright orange solution became dark red. The solution was concentrated to ca. 4 mL and hexane (20 mL) was added. The obtained pale orange solid was filtered off, washed with hexane and vacuum dried. Yield: 75% (109 mg). ^{31}P-NMR (121.42 MHz, 298 K, $CDCl_3$): 57.5 ppm (*d*, ^{1}J(Rh-P) = 101 Hz). ^{1}H-NMR (300 MHz, 298 K, $CDCl_3$): 8.78–7.38 (*m*, 40H, Ph), 2.38 (br, 4H, P–(CH_a)$_2$)-P), 2.27 (br, 4H, P–(CH_bH)$_2$)-P). ESI–MS(+) *m/z*: 501.0 (M − 2CO − 2Cl$^-$, calc.: 501.3). IR (KBr, cm^{-1}): 1986 versus, *v*(C≡O).

Synthesis of $[RhCl(CO)]_2$(μ-dppa)$_2$ **(4a)** A similar procedure that described for **2a** was used in the synthesis of **4a,** but dppa instead of dppe was used to obtain a pale yellow solid. Yield: 70%. ^{31}P-NMR (121.42 MHz, 298 K, $CDCl_3$): 3.6 ppm (*d*, ^{1}J(Rh-P) = 133 Hz). ^{1}H-NMR (300 MHz, 298 K, $CDCl_3$): 7.87–7.25 (m, Ph). ESI–MS(+) *m/z*: 497.0 (M − 2CO − 2Cl$^-$, calc.: 497.2). IR (KBr, cm^{-1}): 2105 m, *v*(C≡C); 1986 versus, *v*(C≡O).

Synthesis of $[RhCl(CO)]_2$(μ-dppbz)$_2$ **(5a)** Similar procedure described for **2a** was used in the synthesis of **5a** using dppbz instead of dppe to obtain a pale yellow solid. Yield: 70%. ^{31}P-NMR (121.42 MHz, 298 K, $CDCl_3$): 62.3 ppm (*d*, ^{1}J(Rh-P) = 134 Hz). ^{1}H-NMR (300 MHz, 298 K, $CDCl_3$): 7.59–6.83 (*m*, Ph + P − C_6H_4 − P). ESI–MS(+) *m/z*: 995.0 ([M–3 Ph]$^+$, calc.: 994.9). IR (KBr, cm^{-1}): 1973 versus, *v*(C≡O).

Synthesis of $[RhCl(CO)]_2$(μ-xantphos)$_2$ **(6a)** Similar procedure described for **2a** was used in the synthesis of **6a** by using xantphos instead of dppe to obtain an orange solid. Yield: 80%. ^{31}P-NMR (121.42 MHz, 298 K, $CDCl_3$): 21.1 ppm (*d*, ^{1}J(Rh-P) = 131 Hz). ^{1}H-NMR (300 MHz, 298 K, $CDCl_3$): 7.59–7.07 (*m*, 56H, Ph + $H_{Arom,Xanthene}$),

1.85–1.55 (*m*, 12H, CH_3). ESI–MS(+) *m/z*: 1491.0 ($M + H^+$, calc.: 1490.9), 1426.1 ($M - CO - Cl^-$, calc.: 1426.6), 710.0 ($M - 2Cl^-$, calc.: 709.6). IR (KBr, cm^{-1}): 1986 versus, $\nu(C\equiv O)$.

Synthesis of $([RhCl(CO)]_2(\mu\text{-}4,4'\text{-bipy}))_2(\mu\text{-dppbz})_4$ **(5b)** A dichloromethane solution (5 mL) of dppbz (37 mg, 0.08 mmol) was added to a solution (5 mL) of $[RhCl(CO)_2]_2(\mu\text{-bipy})$ (22 mg, 0.04 mmol) in the same solvent. After 1 h of stirring, the orange solution turned bright yellow. The solution was concentrated to ca. 4 mL and hexane (15 mL) was added. The obtained pale orange solid was filtered off, washed with hexane and vacuum dried. Yield: 80% (44 mg). ^{31}P-NMR (121.42 MHz, 298 K, acetone-d_6): 61.7 ppm (*d*, ^{1}J(Rh-P) = 133 Hz). ^{1}H-NMR (300 MHz, 298 K, acetone-d_6): 8.90 (br, 8H, $H_{\alpha\text{-pyr}}$), 8.05–7.02 (*m*, 104H, Ph + P − C_6H_4–P + $H_{\beta\text{-pyr}}$). Maldi/TOF *m/z*: 2131.1 (M − dppz − 4CO − 2Cl + H^+, calc.: 2131.0), 1047.0 ($[RhCl(CO)]_2(\mu\text{-dppbz})_2$ − 2-Ph − Cl + CH_3CN, calc.: 1047.1). IR (KBr, cm^{-1}): 2097, 2059 s, 2012 versus, 1978 versus, $\nu(C\equiv O)$; 1612 s, ν(C=N).

Synthesis of $([RhCl(CO)]_2(\mu\text{-}4,4'\text{-bipy}))_2(\mu\text{-xantphos})_4$ **(6b)** Similar procedure described for **5b** was used in the synthesis of **6b** by using xantphos instead of dppbz. Yield: 85%. ^{31}P-NMR (121.42 MHz, 298 K, acetone-d_6): 20.9 ppm (*d*, ^{1}J(Rh-P) = 137 Hz). ^{1}H-NMR (300 MHz, 298 K, acetone-d_6): 8.94 (br, 8H, $H_{\alpha\text{-pyr}}$), 8.08 (*m*, 8H, $H_{\beta\text{-pyr}}$), 7.92–6.83 (*m*, 112H, Ph + $H_{Arom,Xanthene}$), 2.30 (*m*, 24H, $(CH_3)_{2,Xanthene}$). Maldi/TOF *m/z*: 1599.2 ($M - 2Cl^- - CO$, calc.: 1599.1), 1586.2 ($M - 2Cl^- - 2CO$, calc.: 1586.10), 1572.2 ($M - 2Cl^- - 3CO$, calc.: 1572.1), 1557.2 ($M - 2Cl^- - 4CO$, calc.: 1557.1), 1543.3 ($M - 2Cl^- - 4CO - 2\ CH_3$, calc.: 1543.2), 1525.2 ($M - 2Cl^- - 4CO - 4\ CH_3$, calc.: 1525.2), 1510.2 ($M - 2\ Cl^- - 4\ CO - 6\ CH_3$, calc.: 1510.2), 1373.9 (M − xantphos − 2 $Cl^- + CH_2Cl_2 + H_2O$, calc.: 1373.8), 1353.1 (M − xantphos − 2 $Cl^- +$ MeOH + 2 H_2O, calc.: 1353.1), 1322.0 (M − xantphos − 2 Cl^-, calc.: 1322.0). IR (KBr, cm^{-1}): 2099, 2012 s, 1986 m, 1966 w, $\nu(C\equiv O)$; 1612 m, ν(C=N).

Synthesis of $[Rh(CO)_2(dppm)](OTf)$ **(1c)** Solid AgOTf (37 mg, 0.14 mmol) was added to a stirred solution of $[Rh(\mu\text{-}Cl)(CO)_2]_2$ (25 mg, 0.06 mmol) and dppm (49 mg, 0.13 mmol) in CH_2Cl_2 (20 mL). After 15 min stirring, AgCl was eliminated by filtration through Celite, the solution was concentrated and hexane (50 mL) was added and a yellow–orange solid was obtained. Yield: 90% (75 mg). ^{31}P-NMR (121.42 MHz, 298 K, $CDCl_3$): 19.4 ppm (*d*, ^{1}J(Rh-P) = 114 Hz). ^{1}H-NMR (300 MHz, 298 K, $CDCl_3$): 7.70–7.11 (*m*, 20H, Ph), 4.08 (br, 1H, P–CHH_a–P), 3.57 (br, 1H, P–CH_bH–P). ESI–MS(+) *m/z*: 515.3 ($M^+ - CO$, calc.: 515.0). IR (KBr, cm^{-1}) 1970, $\nu(C\equiv O)$; 1101, 1030 (OTf^-).

Synthesis of $[Rh(CO)_2(dppe)](OTf)$ **(2c)** Similar procedure described for **1c** was used in the synthesis of **2c** by using dppe instead of dppm to obtain a pale yellow solid. Yield: 92%. ^{31}P-NMR (121.42 MHz, 298 K, $CDCl_3$): 57.6 ppm (*d*, ^{1}J(Rh-P) = 132 Hz). ^{1}H-NMR (300 MHz, 298 K, $CDCl_3$): 7.33–7.11 (*m*, 20H, Ph), 2.11 (br, 4H, P–CH_2CH_2–P). ESI–MS(+): 453.2 (M^+–CO–Ph, calc.: 453.2). IR (KBr, cm^{-1}) 1972, $\nu(C\equiv O)$; 1101, 1031 (OTf^-).

Synthesis of $[Rh(CO)_2(dppbz)](OTf)$ **(5c)** Similar procedure described for **1c** was used in the synthesis of **5c** by using dppbz instead of dppm to obtain a pale yellow solid. Yield: 94%. ^{31}P-NMR (121.42 MHz, 298 K, $CDCl_3$): 62.4 ppm (*d*, ^{1}J(Rh-P) = 134 Hz). ^{1}H-NMR (300 MHz, 298 K, $CDCl_3$): 7.38–6.75 (*m*, 24H, Ph). ESI–MS(+): 501.3 (M^+–CO–Ph, calc.: 501.3). IR (KBr, cm^{-1}) 1970, $\nu(C\equiv O)$; 1103, 1032 (OTf^-).

Synthesis of $[Rh(CO)_2(xantphos)](OTf)$ **(6c)** Similar procedure described for **1c** was used in the synthesis of **6c** by using xantphos instead of dppm to obtain a pale yellow solid. Yield: 90%. ^{31}P-NMR (121.42 MHz, 298 K, $CDCl_3$): 36.7 ppm (*d*, ^{1}J(Rh-P) = 123 Hz). ^{1}H-NMR (300 MHz, 298 K, $CDCl_3$): 7.83–7.42 (*m*, 26H, Ph), 1.74 (s, 6H, CH_3). ESI–MS(+): 710.1 (M^+–CO, calc.: 710.1). IR (KBr, cm^{-1}) 1974, $\nu(C\equiv O)$; 1101, 1029 (OTf^-).

Catalytic hydrogenation procedure

(E)-4-phenyl-but-3-en-2-one (146 mg, 1.0 mmol) was added to a stirred solution of Rh catalyst (0.01 mmol of rhodium: 6 mg for **1a**, **2a**, **4a** and **5a**; 7.5 mg for **6a**; 6 mg for **2c**; 6.3 mg for **1b**) in ethanol (20 mL) in the presence of decane (142 mg, 1.0 mmol) as internal standard. The solution was then pressurised with H_2 (between 5 and 40 bar) at 50 °C during 6 h. The crude solution was filtered off through Celite and analysed by GC/MS.

Acknowledgements Authors would like to thank Dr. Isabelle Favier and Prof. Montserrat Gómez from the Centre National de la Recherche Scientifique (CNRS) and the Université de Toulouse 3—Paul Sabatier in Toulouse (France) for the catalytic experiments. Financial support from the Ministerio de Economía y Competitividad of Spain (Projects CTQ2012-31335 and CTQ2015-65040-P) are also acknowledged.

References

1. Cook TR, Zheng YR, Stang PJ (2013) Chem Rev 113:734
2. Cook TR, Zheng YR, Stang PJ (2015) Chem Rev 115:7001
3. Smulders MMJ, Riddell IA, Browne C, Nitschke JR (2013) Chem Soc Rev 42:1728
4. Ferrer M, Pedrosa A, Rodríguez L, Rossell O, Vilaseca M (2010) Inorg Chem 49:9438

5. Angurell I, Ferrer M, Gutiérrez A, Martínez M, Rocamora M, Rodríguez L, Rossell O, Lorenz Y, Engeser M (2014) Chem Eur J 20:14473
6. Ferrer M, Gutiérrez A, Rodríguez L, Rossell O, Ruiz E, Engeser M, Lorenz Y, Schilling R, Gómez-Sal P, Martín A (2012) Organometallics 31:1533
7. Alvariño C, Pía E, García MD, Blanco V, Fernández A, Peinador C, Quintela JM (2013) Chem Eur J 19:15329
8. Ferrer M, Gómez-Bautista D, Gutiérrez A, Orduña-Marco G, Oro LA, Pérez-Torrente JJ, Rossell O, Ruiz E (2016) Organometallics 35:336
9. Ferrer M, Gómez-Bautista D, Gutiérrez A, Miranda JR, Orduña-Marco G, Oro LA, Pérez-Torrente JJ, Rossell O, García-Orduña P, Lahoz FJ (2014) Inorg Chem 53:1699
10. Forniés J, Gómez J, Lalinde E, Moreno MT (2004) Chem Eur J 10:888
11. Wang H, Guo XQ, Zhong R, Lin YJ, Zhang PC, Hou XF (2009) J Organomet Chem 694:3362
12. Han YF, Lin YJ, Jia WG, Jin GX (2009) Dalton Trans 2009:2077–2080
13. Álvarez-Vergara MC, Casado MA, Martín ML, Lahoz FJ, Oro LA, Pérez-Torrente JJ (2005) Organometallics 24:5929
14. Wang GL, Lin YJ, Jin GX (2011) Chem Eur J 17:5578
15. Han YF, Jia WG, Lin YJ, Jin GX (2008) J Organomet Chem 693:546
16. Grote Z, Bonazzi S, Scopelliti R, Severin K (2006) J Am Chem Soc 128:10328
17. Han YF, Lin YJ, Weng LH, Berke H, Jin GX (2008) Chem Commun 3:350–352
18. Govindaswamy P, Lindner D, Lacour J, Süss-Fink G, Therrien B (2007) Dalton Trans (39):4457–4463
19. Tran NT, Stork JR, Pham D, Chancellor CJ, Olmstead MM, Fettinger JC, Balch AL (2007) Inorg Chem 48:7998
20. Escárcega-Bobadilla MV, Rodríguez-Pérez L, Teuma E, Serp P, Masdeu-Bultó AM, Gómez M (2011) Catal Lett 141:808
21. Giustra ZX, Ishibashi JSA, Li SY (2016) Coord Chem Rev 314:134
22. Delgado-Rebollo M, Prieto A, Pérez PJ (2014) Chem Cat Chem 6:2047
23. Sarmentero MA, Fernández-Pérez H, Zuidema E, Bo C, Vidal-Ferran A, Ballester P (2010) Angew Chem Int Ed 49:7489
24. Besset T, Norman DW, Reek JNK (2013) Adv Synth Catal 355:348
25. Li Y, Wang Z, Ding K (2015) Chem Eur J 21:16387
26. Vargiu AV, Magistrato A (2012) Inorg Chem 51:2046
27. Mirtschin S, Krasniqi E, Scopelliti R, Severin K (2008) Inorg Chem 47:6375
28. Park J, Hong S (2012) Chem Soc Rev 41:6931
29. Wauchwalter P, Rose J, Braunstein P (2015) Chem Rev 115:28
30. Ho JHH, Wagler J, Willis AC, Messerle BA (2011) Dalton Trans 40:11031
31. Bratko I, Gómez M (2013) Dalton Trans 42:10664
32. Terrade FG, Lutz M, Reek JNH (2013) Chem Eur J 19:10458
33. Kokan Z, Kirin SI (2013) Eur J Org Chem 36:8154–8161
34. Sanhes D, Gual A, Castillón S, Claver C, Gómez M, Teuma E (2009) Tetrahedron Asymmetry 20:1009
35. Bravo MJ, Ceder RM, Muller G, Rocamora M (2013) Organometallics 32:2632
36. Matthews RC, Howell DK, Peng WJ, Train SG, Treleaven WD, Stanley GG (1996) Angew Chem Int Ed Engl 35:2253
37. Ho JHH, Hodgson R, Wagler J, Messerle BA (2010) Dalton Trans 39:4062
38. Freixa Z, Kamer PCJ, Lutz M, Spek AL, van Leeuwen PWNM (2005) Angew Chem Int Ed 44:4385
39. Feliz M, Freixa Z, van Leeuwen PWNM, Bo C (2005) Organometallics 24:2608
40. Rodríguez L, Ferrer M, Rossell O, Coco S (2009) J Organomet Chem 694:3951
41. Lamb G, Clarke M, Slawin AMZ, Williams B, Key L (2007) Dalton Trans 47:5582–5589
42. Lamb GW, Clarke ML, Slawin AMZ, Williams B (2008) Dalton Trans 36:4946–4950
43. Cowie M, Dwight SK (1980) Inorg Chem 19:209
44. López-Vallbuena JM, Escudero-Adan EC, Benet-Buchholz J, Freixa Z, van Leeuwen PWNM (2010) Dalton Trans 39:8560
45. de Pater BC, Frühous HW, Vrieze K, de Gelder R, Baerends EJ, McCormack D, Lutz M, Spek AL, Hartl F (2004) Eur J Inorg Chem 8:1675–1686
46. Kunkely H, Vogler A (1999) J Organomet Chem 577:358
47. Indoli MT, Chiorboli C, Sandola F (2007) Top Curr Chem 280:215
48. Youssef TE (2010) Polyhedron 29:1776
49. Rojas S, Murcia-Mascarós S, Terrero P, García Fierro JL (2001) New J Chem 25:1430
50. Chahdoura F, Pradel C, Gomez M (2013) Adv Synth Catal 355:3648
51. Guyonnet Bilé E, Sassine R, Denicourt-Nowicki A, Launay F, Roucoux A (2011) Dalton Trans 40:6524
52. Hewertso W, Watson HR (1962) J Chem Soc 1490–1494
53. Mague J, Mitchener JP (1969) Inorg Chem 8:119
54. Becke AD (1993) J Chem Phys 98:5648
55. Lee C, Yang W, Parr RG (1988) Rev Phys B 37:785–789
56. Wadt WR, Hay PJ (1985) J Chem Phys 82:284
57. Hay PJ, Wadt WR (1985) J Chem Phys 82:299
58. Hehre WJ, Ditchfield R, Pople JA (1972) J Chem Phys 56:2257